



Galeote-Checa, G., Nabaei, V., Das, R. and Heidari, H. (2020) Wirelessly Powered and Modular Flexible Implantable Device. In: 2020 27th IEEE International Conference on Electronics, Circuits and Systems (ICECS), Glasgow, Scotland, 23-25 Nov 2020, ISBN 9781728160450 (doi:[10.1109/ICECS49266.2020.9294856](https://doi.org/10.1109/ICECS49266.2020.9294856)).

This is the author's final accepted version.

There may be differences between this version and the published version. You are advised to consult the publisher's version if you wish to cite from it.

<http://eprints.gla.ac.uk/223330/>

Deposited on: 22 September 2020

Enlighten – Research publications by members of the University of Glasgow  
<http://eprints.gla.ac.uk>

# Wirelessly Powered and Modular Flexible Implantable Device

Gabriel Galeote-Checa, Vahid Nabaei, Rupam Das, Hadi Heidari  
Microelectronics Lab (meLAB), James Watt School of Engineering, University of Glasgow, G12 8QQ, UK  
Hadi.Heidari@glasgow.ac.uk

**Abstract**—This paper presents a novel configuration for wirelessly powered and modular implantable device fabricated on flexible electronics. This Wireless Power Transfer based neural implant consist of receiver antenna, power management circuit, and shank for power transmission, recording and stimulation. Here, the novelty of the implementation falls on the modularity concept providing two different configurations that helps on the customization of the implant, e.g. for different shank lengths or antenna designs. For such modular design, two antennas were designed, one of 13.56 MHz and another of 8 MHz that were tested electrically to measure the amount of energy received in the receiver side and corroborate the correct performance of the power transmission system. Both, electrical and mechanical analysis are provided to prove the correct operation of the fabricated device under the modelled environment. COMSOL Multiphysics was used to model mechanical behavior of device and find optimal material among a dataset of materials that are commonly used for flexible implantable devices. As a result, Parylene C, with von mises stress of 179Mpa in bent working condition, was found as the most suitable material. Although Parylene C is the optimal material from mechanical point of view, in this paper polyimide is chosen for the final fabrication of the device due to its availability and cost-effectiveness, which provides adequate implant-brain tissue mechanical, biocompatibility and biointegration

**Keywords**— Flexible, Polyimide, Implantable electronics, Modular design and Wireless Power Transfer.

## I. INTRODUCTION

The optimal design of implantable devices requires to take into account several factors that highly restrict the options available in terms of biocompatibility, biointegration and long-term operation. In addition, stimulation target site and technique used, type and pathology to be treated among others are constraints that difficult the approach to the design of such devices. More specifically, cranial structure limits the access to the brain adding complexity to the design considerations. The recovery period after the surgery, invasiveness of the implantation procedure and feasibility of the medical surgery and long term operation are critically determined by the size, flexibility, material choice and shape of the implant [1-4]. In addition to the foregoing, the viscoelasticity of the brain tissue presents a serious quandary. While increasing the robustness of the implant encapsulation and materials could be initially considered as desirable, in the practice this would trigger a foreign body reaction as a result of mechanical mismatch resulting on body rejection to the implant [4, 5]. Force and tissue insertion dimpling are two factors to consider in the design of the implant because implantation should remain

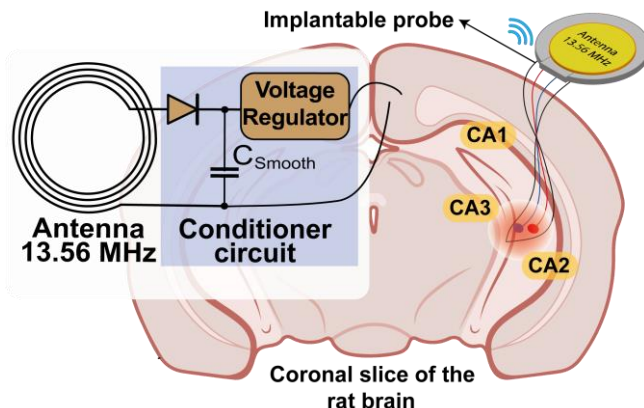


Fig. 1. Conceptual model of the implantable device with the proposed mechanical design in similar implantation case. The electronic design follows a modular approach consisting of three sections: Antenna, Conditioner Circuit and Shank.

intact the surrounding tissue as much as possible [1, 2]. And finally, the apparent recording site impedance of the surrounding tissue which can vary during the weeks after implantation damaging the operation of the bioimplantable device. Addressing what was commented before, the difficult access to the brain tissue could be overcome by using wireless power transmission (WPT). For the mechanical matching to the brain tissue, new approaches of flexible circuits are being used reporting satisfactory results [1, 2]. This option is in fact the most interesting as it is possible to reduce the foreign body response, as reported in other author's studies[6, 7].

Latest advances in Wireless Power Transmission (WPT) systems have provided new opportunities for powering of fully implantable devices[4, 8, 9]. These techniques for wireless energy harvesting achieves some capabilities that are especially important for the design of brain implants, avoiding the negative effects of wire-based powering systems as well as other numerous benefits like low size or better geometry for biocompatibility [4, 9-11]. WPT systems are advantageous over the conventional battery-based implants, due to the higher degree of freedom and ease of use in operation. Moreover, WPT allows for long term biological integration and chronic implantation [4, 5]. Figure 1 shows the configuration of the proposed device for this work illustrating the idea of a wireless device that uses an electromagnetic antenna for power reception.

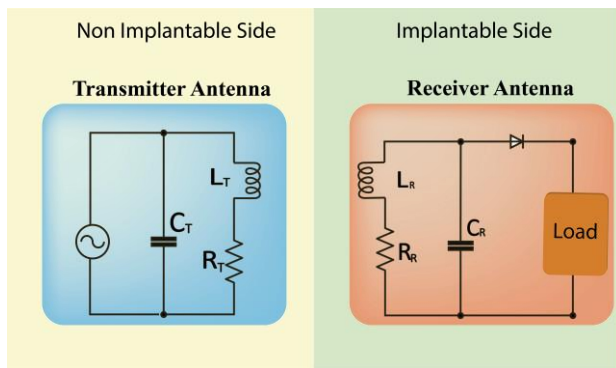


Fig. 2. Schematic diagram of a WPT between two inductively coupled antenna system in a parallel resonant circuit for a general load. The receiver side is implanted in the brain while the transmitter side could be attached under or over skin.

Special mention to the field of flexible materials and 3D surfaces that has represented a big opportunity for the field of brain implantable devices due to the excellent mechanical properties that provide better biocompatibility with the brain tissue [12, 13]. The main advantage of this new approach is the improvement of the biological long-term viability of the implant as the gap of mechanical mismatch between the brain tissue and the device is reduced so far. Despite the attractive opportunity of flexible circuits, electronic designs over bendable substrates present special difficulties related to fabrication over large areas and integration on diverse flexible substrates. Other restrictions in flexible circuits are the reliability and uniform operation of flexible integrated circuits under various bending states [12]. Thus, proper miniaturization of the circuit and components is desirable in order to reduce this effect.

Here, a fully implantable, flexible, and wirelessly powered device is proposed following a modular approach where every module can be modified independently while satisfying the electrical and mechanical requirements of the design. Here, modularity is understood as independent designs that are assembled together, thus giving the option of changing one of the modules while remaining intact the rest of it (e.g. use other different antenna for WPT like ultrasonic WPT or other conditioning circuit). The high flexibility, wireless power harvesting, and tiny electrical circuit allow this implant to be adapted for both, soft injectable electrodes and/or light stimulation [14]. Additionally, mechanical analysis have been carried out in COMSOL Multiphysics to investigate mechanical behaviour of the device in bend working condition and implantation phase. For this purpose, two parameters of device von mises stress and safety factor have been studied to choose optimal design from mechanical points of view. The implant is divided into three parts: (i) WPT system for the wireless power harvesting of the implant; (ii) conditioner circuit for the AC/DC conversion; and (iii) a shank for testing the performance of the WPT. An illustrative model of this proposal is shown in Fig. 1. To corroborate the theoretical model and the real fabrication, the device was fabricated in Dupont substrate reporting satisfactory results.

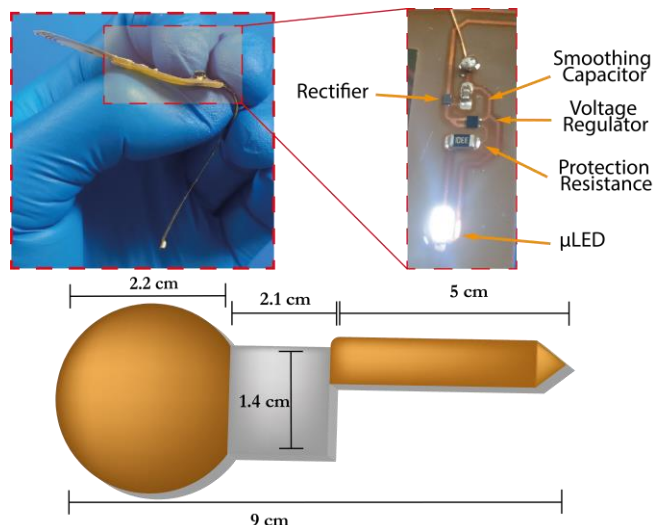


Fig. 3. Fabricated device on similar mechanical implantation case zooming on the electronic design with components up to 1 mm size on Dupont Pyralux substrate. The device is powered while implantation case showing the successful lighting of the LED.

## II. METHODOLOGY

The novelty of this device is based on the concept of modularity. While most of other current available works are ad-hoc designs [9, 14]. herein, the proposed device consists of three independent modules: Wireless power transmission, Signal Conditioning and shank. Those modules are interchangeable with other designs as electronic independency is satisfied. The WPT is enabled through inductive loop. There are two typologies of magnetic WPT: inductive and capacitive coupling [15]. In inductively coupled wireless power transmission systems the inductance of one of the antennas, typically the transmitter, is designed or measured empirically and then, the other antenna, normally the receiver, is designed in order to match the same resonant frequency and consequently, inductance. The resonant frequency of an antenna is strongly determined by the geometry. However, in some cases, it is better to design the geometry of transmitter and receiver coils and match them through capacitance, mitigating the effect of the imaginary part of the antenna's inductance. The equivalent circuit of an antenna is as shown in Fig. 2, from where the capacitance could be calculated straight forward for capacitive matching. In this work, two antennas were designed to prove the modular concept of the implant. An antenna of 13.56 MHz was designed for the final prototype and another antenna of 8 MHz for testing. The parameters of the 13.56 and 8 MHz antenna designed are shown in Table 1. The 13.56 MHz was design by a circular geometry while the 8 MHz antenna follows a square design, also to prove different geometric configurations. The 8 MHz antenna was inductively coupled but the 13.56 MHz needed tuning. For that, the theoretical inductance of the 13.56 MHz coil was calculated as 0.992  $\mu$ H. Then, the matching capacitance of 138 pF to tune the receiver coil at 13.56 MHz. The 13.56 MHz antenna is shown in Fig. 3.

The signal conditioner module consists of two parts: a half-wave rectifier and voltage regulator. The half-wave rectifier,

made by a simple one-diode half-wave set-up, allows an electric current to pass in only one direction. Consecutively, a smoothing capacitor is implemented to regulate the sharpness of the sine wave and create a more stable signal. The half-wave rectifier consists of a Schottky diode (NSR05F40NXT5G) with a low forward voltage drop of maximum 500 mV connected to a smoothing capacitor (2.2 nF) in parallel, as shown in Fig. 1. After the rectification and smoothing of the signal, a linear Low-Dropout Voltage Regulator (NCP161) was implemented. The fabricated circuit is shown in Fig. 3, illustrating the dimensions and configuration of the fabricated final design.

TABLE I. GEOMETRIC PARAMETERS OF DESIGNED ANTENNAS.

13.56 MHz Antenna	
Outer Diameter ( $\varnothing_{out}$ )	22.3 mm
Inner Diameter ( $\varnothing_{in}$ )	12.3 mm
Wire Width	0.5 mm
Wire Spacing	0.5 mm
8 MHz Antenna	
Outer Diameter ( $\varnothing_{out}$ )	51 mm
Inner Diameter ( $\varnothing_{in}$ )	41 mm
Wire Width	0.5 mm
Wire Spacing	0.5 mm

The shank of the device is the most flexible section to provide fully biointegration and mechanical matching to the neural interface. For achieving that, a model with a long shank (5 cm) was designed, with two copper traces, one for input and other for ground, that end up in the LED at the tip of the shank. Due to the modular design, we can use any kind of shank length and LEDs while it keeps the same electrical properties specified in the last section. The most important consideration for the design of the shank is to control the length of it in order to have a correct power input in the terminal side of it.

For the fabrication of the device polyimide was chosen for this work due to availability and cost-effectiveness, and also because it provides adequate implant-brain tissue mechanical, biocompatibility and biointegration. The used polyimide was Dupont Pylarlux AP8535R. The substrate has a thickness of 75  $\mu\text{m}$  and a copper thickness of 18  $\mu\text{m}$ . For the fabrication, it was carried out the typical chemical etching process using the etchant Ferric Chloride. However, a dataset off 5 materials (Si, Cu, Polyimide, SU-8, Parylene-C and PDMS) was chosen for a mechanical simulation run in COMSOL Multiphysics to investigate which other materials might show better mechanical properties than polyimide. Von mises stress tests were investigated in that section.

### III. ELECTRICAL ANALYSIS

To check the electrical behavior of the circuit two experiments were carried out: power over distance and Power Spectral Density (PSD) analysis. In the first experiment, a transmitter coil and receiver coil are coupled and then, the power on the shank is measured while the implant is moved from 0 to 7 cm with a step of 0.5 cm. The second experiment consists of doing a frequency sweep from 0 to 14 MHz, measuring the output power after the voltage regulator in both devices, 13.56 MHz and 8 MHz. Data obtained (Fig. 4a) have reported a maximum transmission range of 6 cm for the 13.56 MHz antenna with a

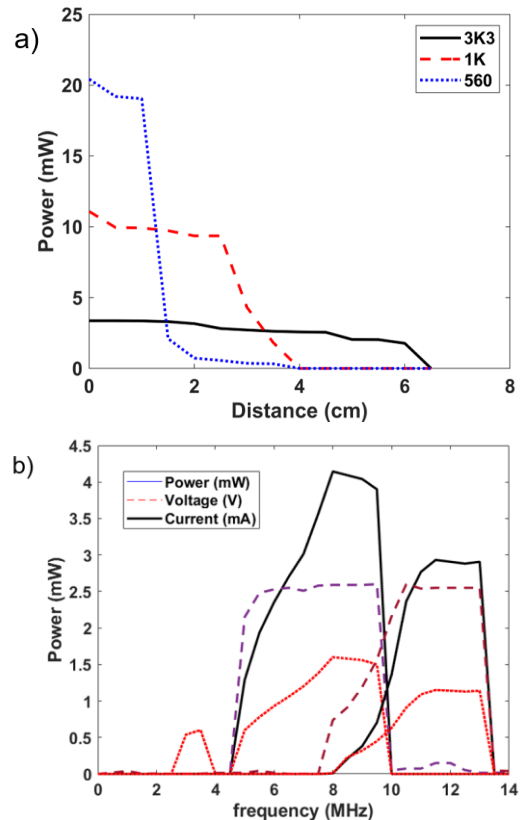


Fig. 4. a) Power variations depending on the distance with different protecting resistances. b) Power Density Spectrum for antennas of 8 MHz and 13.56 MHz.

resistance of 3K3 Ohm. Regarding the second experiment, the power spectrum density (Fig. 4b) shows that both antennas have their resonant frequencies at 13.56 MHz and 8 MHz respectively. Note that the LED is powered successfully during the power transmission and due to the voltage regulator (LDO. In [9] and [11], similar results are achieved proving the correct power obtained in the shank of this device.

### IV. MECHANICAL ANALYSIS

In this section, we have performed mechanical characterization to find device optimal design from mechanical point of view. The opto-electronic device has been modelled introducing a Parylene C based substrate and copper wirings on it. The material properties of Parylene C and copper have been presented in Table 1. In the developed model for this device, the total length of the device is 9 cm and the shank is 5 cm long, with 6 mm width. Those dimension follows a work of miniaturization, but the shank is built long to probe mechanical properties of the Polyimide and electric circuit printed on it. The thicknesses of the device substrate (Parylene C) and copper wire are 75  $\mu\text{m}$  and 18  $\mu\text{m}$ , respectively. To investigate mechanical behaviour of the proposed opto-electronic device in bent condition, von mises stress and safety factor have been calculated for the applied perpendicular and axial loads to the device plane, respectively. A 3D modelling based on finite element method (FEM) has been carried out using COMSOL Multiphysics. To mimic the

bend working condition, a vertical loading force is applied gradually on the shank plane to bend it, to achieve the conformation that represents opto-electronic device working condition after implantation (see Fig. 5a). The values of von mises stress have been calculated when the tip maximum displacement reaches to 42 mm. As seen from simulation result in Fig. 5a, the point with maximum von mises stress of  $8.043 \times 10^9$  Pa is in the copper wire in the knee part of the bent device because the copper has higher Young's modulus compared to Parylene C.

The proposed design for the device should also provide lateral flexibility and axial stiffness to survive the mechanical forces experienced during insertion. This enables successful tissue penetration without the need for implantation stylus or similar stiffening devices. To investigate this, device safety factor, as an important criterion for the insertion, has been calculated applying an axial load to the device base (circle part) and

fixing the tip of the shank (see Fig. 5b). Safety factor for axial loading is calculated by comparing yield stress strength and von mises stress, using

$$Safety\ factor = \frac{(yield\ stress)}{(von\ mises\ stress)} \quad (1)$$

As can be seen from simulation results from Fig. 5b, for this device the maximum von mises stress is obtained 97.69 MPa, considering yield stress value of 510 MPa for the copper, therefore the obtained safety factor for this device is 5.32. The accepted safety factor value is equal to or greater than 5 [16].

To investigate device mechanical behavior from material point of view, substrate of the device has been modelled using different polymers including: polydimethylsiloxane (PDMS), Parylene C, SU-8 and Polyimide (PI). Properties of these polymers as well as the silicon (Si), as a reference and stiff material, are presented in Table 1. The von mises stress values in 90° bend working condition of the device have been calculated for substrate made by different polymers and compared to each other (see Fig. 6). As it can be seen from Fig. 6, the lowest stress can be obtained using PDMS instead of PI, where the von mises stress can be considerably reduced from 224 MPa to 0.046 MPa. But, one of the important factors that should be considered for this device is required stiffness for insertion. The device substrate made by PDMS will not survive insertion force in implantation stage. Furthermore, though PDMS exists in medical class, that meets both USP class VI and ISO 10993, it has been reported that the curing agent might be toxic [17]. Therefore, among the investigated polymers, Parylene C can be chosen as the most suitable material for the device substrate which shows lowest stress during the device working condition.

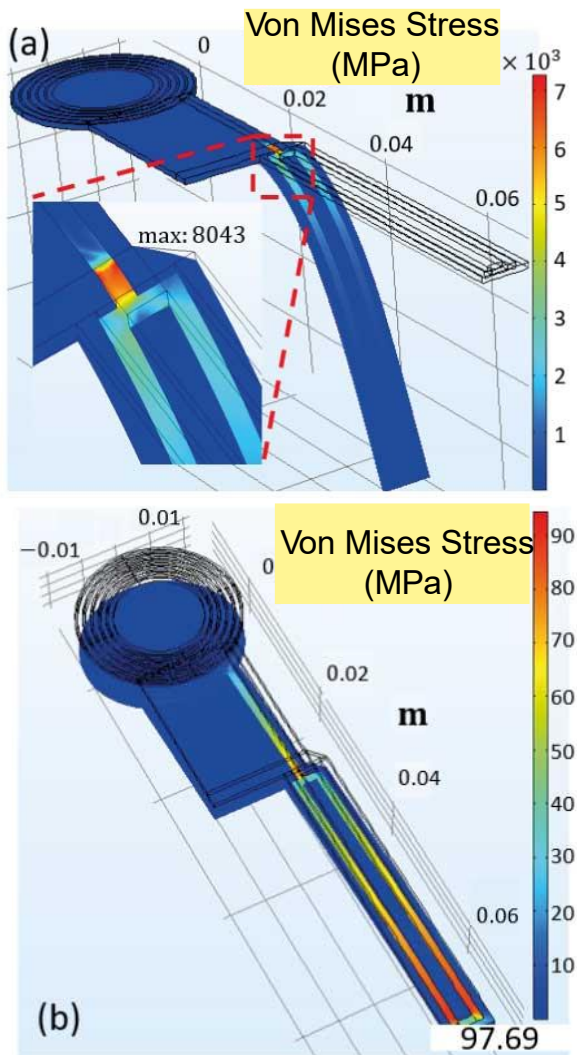


Fig. 5. Simulation result for (a) von mises stress analysis in bent working condition of the device, the point with maximum von mises stress of  $8.04 \times 10^9$  Pa is located in the copper wire, (b) calculation of the safety factor to investigate device mechanical behavior during the insertion, obtained safety factor for this device is 5.32.

TABLE II. Device material properties.

Material	Young's Modulus [GPa]	Poisson's Ratio	Density [kg/m <sup>3</sup> ]
Si	185	0.28	2330
Cu	135	0.35	8300
PI	3.1	0.37	1300
SU-8	2.87	0.22	1190
Parylene C	2.76	0.4	1289
PDMS	$7.5 \times 10^{-4}$	0.5	965

## V. CONCLUSION

In this work, a new design approach of implantable devices is proposed, using the concept of modularity. This modularity aims to achieve customization of implants for everyone's case. The device was divided into three modules: Wireless Power Transmission stage, signal conditioning and shank. These modules can be redesigned using different WPT systems, conditioning circuits and shanks for various stimulation methods and designs. Two antennas were designed for the WPT system of this device, one for 13.56 MHz and another for 8 MHz. The signal conditioning unit implemented is made of a one-diode half-wave rectifier set up. The fabrication of

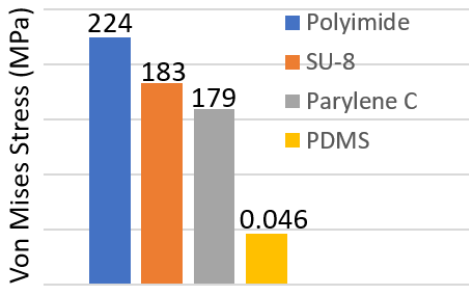


Fig. 6. Simulation results for calculation of von mises stress for the device substrate made by different polymers.

the device was carried out in polyimide Dupont Pyralux AP8535R. The implant was electrically tested obtaining a maximum transmission distance of the antenna of 13.56 MHz at 6 cm that proves the correct performance of the control circuit. Also, the power density spectrum (PDS) of both, 8 and 13.56 MHz was measured providing reasonable results according to the works of [9 -11]. Finally, the simulations carried out in COMSOL Multiphysics to investigate device mechanical properties reported a safety factor of 5.32 for the material choice during implantation case.

#### ACKNOWLEDGEMENT

This work was supported by the EU H2020 Hybrid Enhanced Regenerative Medicine Systems (HERMES, GA n.824164).

#### REFERENCES

- [1] A. Lecomte, E. Descamps, and C. Bergaud, "A review on mechanical considerations for chronically-implanted neural probes," *J Neural Eng*, vol. 15, p. 031001, Jun. 2018.
- [2] D. Prodanov and J. Delbeke, "Mechanical and Biological Interactions of Implants with the Brain and Their Impact on Implant Design," *Front Neurosci*, vol. 10, p. 11, 2016.
- [3] V. Nabaei, G. Panuccio, and H. Heidari, "Computational Modelling of Brain Implantable Microprobes for Diminishing Micromotions Failure," *12th FENS Forum of Neuroscience*, 11-15 Jul. 2020.
- [4] R. Das, F. Moradi, and H. Heidari, "Biointegrated and Wirelessly Powered Implantable Brain Devices: A Review," *IEEE Trans Biomed Circuits Syst*, vol. 14, pp. 343-358, Apr. 2020.
- [5] G. Galeote-Checa, Uke, K., Sohail, L., Das, R. and Heidari, H. , "Flexible Wirelessly Powered Implantable Device," presented at the International Conference on Electronics Circuits and Systems, Genova, Italy, 27-29 Nov. 2019.
- [6] T. D. Kozai, A. S. Jaquins-Gerstl, A. L. Vazquez, A. C. Michael, and X. T. Cui, "Brain tissue responses to neural implants impact signal sensitivity and intervention strategies," *ACS Chem Neurosci*, vol. 6, pp. 48-67, Jan. 2015.
- [7] H. C. Lee, F. Ejserholm, J. Gaire, S. Currlin, J. Schouenborg, L. Wallman, *et al.*, "Histological evaluation of flexible neural implants; flexibility limit for reducing the tissue response?," *J Neural Eng*, vol. 14, no. 3, Jun. 2017.
- [8] S. Zuo, H. Heidari, D. Farina, and K. Nazarpour, "Miniaturized magnetic sensors for implantable magnetomyography," *Advanced Materials Technologies*, vol. 5, p. 2000185, 2020.
- [9] J. S. Ho, A. J. Yeh, E. Neofytou, S. Kim, Y. Tanabe, B. Patlolla, *et al.*, "Wireless power transfer to deep-tissue microimplants," *Proc Natl Acad Sci U S A*, vol. 111, pp. 7974-9, Jun 3 2014.
- [10] R. Das and H. Yoo, "A multiband antenna associating wireless monitoring and nonleaky wireless power transfer system for biomedical implants," *IEEE Transactions on Microwave Theory and Techniques*, vol. 65, pp. 2485-2495, 2017.
- [11] P. Gutruf, V. Krishnamurthi, A. Vázquez-Guardado, Z. Xie, A. Banks, C.-J. Su, *et al.*, "Fully implantable optoelectronic systems for battery-free, multimodal operation in neuroscience research," *Nature Electronics*, vol. 1, p. 652, 2018.
- [12] H. Heidari, N. Wacker, and R. Dahiya, "Bending induced electrical response variations in ultra-thin flexible chips and device modeling," *Applied Physics Reviews*, vol. 4, p. 031101, 2017.
- [13] S. I. Park, D. S. Brenner, G. Shin, C. D. Morgan, B. A. Copits, H. U. Chung, *et al.*, "Soft, stretchable, fully implantable miniaturized optoelectronic systems for wireless optogenetics," *Nat Biotechnol*, vol. 33, pp. 1280-1286, Dec. 2015.
- [14] J. S. Ho, A. J. Yeh, E. Neofytou, S. Kim, Y. Tanabe, B. Patlolla, *et al.*, "Wireless power transfer to deep-tissue microimplants," *Proceedings of the National Academy of Sciences*, vol. 111, pp. 7974-7979, 2014.
- [15] J. Zhao, K. O. Htet, R. Ghannam, M. Imran, and H. Heidari, "Modelling of Implantable Photovoltaic Cells Based on Human Skin Types," in *2019 15th Conference on Ph. D Research in Microelectronics and Electronics (PRIME)*, 2019, pp. 253-256.
- [16] S. R. I. Gabran, M. T. Salam, J. Dian, Y. El-Hayek, J. L. P. Velazquez, R. Genov, *et al.*, "3-D Flexible Nano-Textured High-Density Microelectrode Arrays for High-Performance Neuro-Monitoring and Neuro-Stimulation," *Ieee Transactions on Neural Systems and Rehabilitation Engineering*, vol. 22, pp. 1072-1082, Sep 2014.
- [17] J. N. Lee, X. Jiang, D. Ryan, and G. M. Whitesides, "Compatibility of mammalian cells on surfaces of poly(dimethylsiloxane)," *Langmuir*, vol. 20, pp. 11684-11691, Dec 21 2004.